

Final state interaction in the reaction $NN \rightarrow \eta NN$

A. Fix* and H. Arenhövel

Institut für Kernphysik, Johannes Gutenberg-Universität Mainz, D-55099 Mainz, Germany

(Dated: October 29, 2018)

The production of η mesons in NN collisions in the near threshold region is analyzed with special emphasis on the role of final state interaction which is calculated using three-body scattering theory. The three-body aspects are shown to be very important in interpreting experimental results for the total cross section of $pp \rightarrow \eta pp$. Furthermore, energy spectra and angular distributions of the emitted particles are calculated and compared to experimental data.

PACS numbers: 13.60.Le, 21.45.+v, 25.20.Lj

I. INTRODUCTION

The production of η mesons in two-nucleon collisions depends strongly on the final state interaction (FSI) as has been stressed in previous work [1, 2, 3, 4, 5, 6]. Notwithstanding this fact, the interaction between the final particles was treated in quite an approximate way. Only the NN interaction has been considered in a more precise manner. The interaction of the η meson either was not considered at all or simulated by means of a Watson enhancement factor. In view of this apparent lack of a correct treatment of FSI we want to study this reaction by using a rigorous three-body model.

The properties of the ηNN system, containing three free particles in the asymptotic region, were investigated in [7] where FSI effects in $\eta - d$ reactions as well as in η photoproduction on a deuteron were studied. As was shown in detail, the three-body aspects of FSI are very important, at least near the threshold region where S waves give by far the largest contribution to the production process. It is obvious that the three-body S wave part is most sensitive to FSI in view of the dominance of the S wave interaction in the NN and ηN subsystems at low energies. Furthermore, it is intuitively clear that primarily the central region of the system, where S waves dominate, is distorted by multiple scattering events. As a consequence, close to threshold the ηNN interaction strongly enhances the $\gamma d \rightarrow \eta np$ cross section. At higher energies, where the large spatial extension of the deuteron comes into play, an essential fraction of higher partial waves contributes increasingly to the η production mechanism. This rapidly reduces the relative S wave contribution to the reaction amplitude, so that the role of FSI diminishes considerably with increasing energy. As a result, already in the region of c.m. excess energies above 100 MeV the behavior of the cross section is well explained in the plane wave approximation for the final state [8].

Turning now to the process $NN \rightarrow \eta NN$, firstly we would like to note that in this case the influence of FSI must be even more important. Here the characteristic radius R of the reaction, determined by $R \sim 1/q$ with q as typical momentum transfer, is only about 0.3 fm. This value is much smaller than in photoproduction, where not too close to the threshold the characteristic range is given by the deuteron radius r_d , i.e., $R \sim r_d \approx 2$ fm. Therefore, one may expect that for energies for which $pR < 1$ is valid, with p denoting the maximal c.m. momentum of the final particles, the final state will be dominated by S waves, for which the role of the ηNN interaction is crucial. Indeed, as will be shown below, in the region from threshold up to an excess energy $Q = 60$ MeV, the contribution of higher partial waves in the final state is of much minor importance compared to the S wave contribution. In this connection, the reaction $NN \rightarrow \eta NN$ seems in general to be more suited for studying the interaction in the ηNN system than η photoproduction, where FSI has a smaller influence. This advantage is however strongly reduced by a poor knowledge of the η production mechanism in NN collisions.

In the present paper we investigate the reactions $np \rightarrow \eta np$ and $pp \rightarrow \eta pp$ in the region of excess energy up to $Q = 60$ MeV which is covered in recent experiments as well as in theoretical studies (see e.g. [9] and references therein). The two questions which we address here are:

(i) To what extent are the three-body aspects essential for a quantitative description of FSI? As was already stressed in [10], the importance of a three-body treatment of FSI is dictated by the proximity of a virtual pole in the ηNN amplitude to the physical region [11]. Because of this property a perturbative approach to the ηNN dynamics, where only the interactions in the two-body NN and ηN subsystems are taken into account, is of little use. In the present study we would like to demonstrate this fact for η production in NN collisions.

* On leave of absence from Tomsk Polytechnic University, 634034 Tomsk, Russia

(ii) What is the role of higher NN partial waves? According to Nakayama [12], the puzzling second bump in the pp invariant mass distribution of $pp \rightarrow \eta pp$ measured at $Q = 41$ MeV in [13] could be understood as arising mostly from a contribution of the 3P_0 state of the final nucleon pair. However, the size of P wave contribution appears to be comparable with that of the 1S_0 one (see e.g. Fig. 4 in [12]). Such a large P wave effect in the region where the NN c.m. kinetic energy is limited to $T_{NN} < Q = 41$ MeV (and in fact the maximum of the distribution of T_{NN} is located at even a considerably lower value because of the preference of higher η momenta) is quite surprising. Therefore, we have investigated again the influence of S , P , and D partial NN waves in both isospin states using the Paris NN potential. Another point, closely connected to this, is the role of the short range behaviour of the NN interaction which is enhanced by quite large momentum transfers accompanying the η production. As will be shown below, this leads in particular to an important role of the tensor force in the final np triplet state for $np \rightarrow \eta np$ because the 3D_1 state, excited in the η production process, couples to the 3S_1 partial wave during subsequent NN rescattering.

First we review briefly in the next section the most essential formal ingredients on which our calculation is based. For the driving $NN \rightarrow NN^*$ transition potential we take a meson exchange model including π , ρ , and η exchanges. The two-body ηN and NN interactions are parametrized in terms of separable t matrices. The dominant S wave part of the ηNN wave function is calculated using three-body scattering theory. In Sect. III our results are compared with experimental data and in Sect. IV the most important conclusions are summarized. In an appendix we list detailed expressions for the $NN \rightarrow NN^*$ amplitude.

II. FORMAL INGREDIENTS

In the center of mass system the reaction to be studied reads in detail

$$N(E, \vec{p}) + N(E, -\vec{p}) \rightarrow N(E_1, \vec{p}_1) + N(E_2, \vec{p}_2) + \eta(\omega_\eta, \vec{q}), \quad (1)$$

where the energies and momenta of the participating particles are explicitly defined for later purpose. The reaction is governed by the transition matrix element

$$M_{TM_T, S' M'_S, SM_S} = \langle \vec{q}; \vec{p}_1, \vec{p}_2; S' M_{S'}; TM_T | \hat{M} | SM_S; TM_T, \vec{p} \rangle, \quad (2)$$

where initial and final states are characterized by the total spin $S(S')$ and isospin T of the nucleon pair. The calculation is done in the region of c.m. excess energy Q up to 60 MeV. Thus the use of nonrelativistic expressions for the energies of the final particles is justified, whereas for the initial state relativistic expressions are taken.

The c.m. cross section for $pp \rightarrow \eta pp$ is then given by

$$\frac{d\sigma}{dq d\Omega_q d\Omega_p} = \frac{1}{(2\pi)^5} \frac{M_N^3 q^2 p_r}{4W m_{\eta p}} \frac{1}{4} \sum_{S' M'_S, SM_S} |M_{11, S' M'_S, SM_S}|^2, \quad (3)$$

where the relative momentum of the two final nucleons $\vec{p}_r = (\vec{p}_1 - \vec{p}_2)/2$ is introduced. The factor $\frac{1}{4}$ results from the average over initial spin states. The corresponding $np \rightarrow \eta np$ cross section is obtained from (3) by the substitution

$$M_{11, S' M'_S, SM_S} \rightarrow \frac{1}{2} \sum_{T=0,1} M_{T0, S' M'_S, SM_S}. \quad (4)$$

For the η production mechanism we have adopted the usual model where first an N^* resonance is excited on one of the nucleons which subsequently decays into the ηN channel. The submatrix M_{NN^*} associated with the transition $NN \rightarrow NN^*$ is expressed as a linear combination of eight pseudoscalar operators Σ_j ($j = 1, 8$) built from the vectors \vec{p} , \vec{p}' , and spin operators $\vec{\sigma}_1$ and $\vec{\sigma}_2$

$$M_{NN^*}(\vec{p}, \vec{p}') = \sum_{j=1}^8 M_j \Sigma_j(\vec{p}, \vec{p}', \vec{\sigma}_1, \vec{\sigma}_2), \quad (5)$$

where \vec{p}' denotes the relative momentum of the NN^* system. The amplitudes M_j are functions of only $p = |\vec{p}|$, $p' = |\vec{p}'|$ and $\vec{p} \cdot \vec{p}'$, and their specific form depends on the model for the η production mechanism. For the operators Σ_j we have chosen the following forms

$$\begin{aligned} \Sigma_{1(2)} &= \vec{\sigma}_1 \cdot \vec{p}^{(\prime)}, \\ \Sigma_{3(4)} &= \vec{\sigma}_2 \cdot \vec{p}^{(\prime)}, \end{aligned}$$

$$\begin{aligned}\Sigma_{5(6)} &= \frac{i}{2}(\vec{\sigma}_1 \times \vec{\sigma}_2) \cdot \vec{p}^{(\prime)}, \\ \Sigma_{7(8)} &= i\sqrt{5} \left\{ (\vec{\sigma}_1 \otimes \vec{\sigma}_2)^{[2]} \otimes (\vec{p}^{(\prime)} \otimes (\vec{p} \times \vec{p}'))^{[2]} \right\}^{[0]}.\end{aligned}\quad (6)$$

The latter two operators are tensor operators in two-nucleon spin space describing a spin transfer of 2 in the transition to the NN^* state. For the impulse approximation (IA), where FSI is ignored, the amplitude $M_{TM_T, S'M'_S, SM_S}$ (2) is given by

$$\begin{aligned}M_{TM_T, S'M'_S, SM_S}^{(\text{IA})} &= \langle S'M_{S'}; TM_T | \left[\left(M_{NN^*}(\vec{p}, \vec{p}_2) - (-1)^{S+T} M_{NN^*}(-\vec{p}, \vec{p}_2) \right) F_{N^*}(\vec{q}, \vec{p}_1) \right. \\ &\quad \left. - (-1)^{S'+T} \left(M_{NN^*}(\vec{p}, \vec{p}_1) - (-1)^{S+T} M_{NN^*}(-\vec{p}, \vec{p}_1) \right) F_{N^*}(\vec{q}, \vec{p}_2) \right] | SM_S; TM_T \rangle.\end{aligned}\quad (7)$$

Here the function $F_{N^*}(\vec{q}, \vec{p})$ describes the propagation of the NN^* configuration followed by the decay $N^* \rightarrow \eta N$.

With respect to the spin structure of the amplitude, only three types of transitions are possible, namely $S = 0 \rightarrow S' = 1$, $S = 1 \rightarrow S' = 0$, and $S = 1 \rightarrow S' = 1$. The transition $S = 0 \rightarrow S' = 0$ is excluded since it does not conserve parity. It is easily seen that the operators Σ_1 through Σ_4 contribute to all three types of transitions. The operators Σ_5 and Σ_6 , being antisymmetric under exchange of $\vec{\sigma}_1$ and $\vec{\sigma}_2$, appear only in channels with a change of spin, i.e. $S = 0 \rightarrow S' = 1$ and $S = 1 \rightarrow S' = 0$, whereas Σ_7 and Σ_8 , which require flipping of the spins of both nucleons, contribute only to $S = 1 \rightarrow S' = 1$.

At low energies, the channel $S = 1 \rightarrow S' = 0$ is strongly favored in the $pp \rightarrow \eta pp$ reaction since it allows the final nucleons to be left in a relative S wave whose contribution is further increased by FSI. For the reaction $np \rightarrow \eta np$ both spin changing transitions are possible near threshold. Apart from a trivial isospin factor 3 appearing for $T = 0$, their relative importance depends crucially on the interference between π and ρ exchange [2]. The transition $S = 1 \rightarrow S' = 1$, which requires either the nucleons to be in a relative P state or the η meson to be emitted at least in a P state is suppressed at low energies.

After these more formal considerations we will now turn to the outline of the η production model used in the present work. The η production mechanism via N^* excitation through meson exchange was considered in a variety of previous studies [1, 2, 3, 4, 5]. In the present work, we have adopted this approach including only π , ρ , and η mesons whose contributions was investigated in greater detail than those of ω , σ and other mesons. The corresponding Lagrangians are taken in the customary form

$$\begin{aligned}\mathcal{L}_{\pi NN} &= i g_{\pi NN} F_{\pi}(q^2) \bar{u}(\vec{p}') \gamma^5 u(\vec{p}) \vec{\tau} \cdot \vec{\phi}_{\pi}, \\ \mathcal{L}_{\pi NN^*} &= g_{\pi NN^*} F_{\pi}^*(\vec{q}_{\pi N}^2) \bar{u}(\vec{p}') u(\vec{p}) \vec{\tau} \cdot \vec{\phi}_{\pi}, \\ \mathcal{L}_{\eta NN} &= i g_{\eta NN} F_{\eta}(q^2) \bar{u}(\vec{p}') \gamma^5 u(\vec{p}) \phi_{\eta}, \\ \mathcal{L}_{\eta NN^*} &= g_{\eta NN^*} F_{\eta}^*(\vec{q}_{\eta N}^2) \bar{u}(\vec{p}') u(\vec{p}) \phi_{\eta}, \\ \mathcal{L}_{\rho NN} &= F_{\rho}(q^2) \bar{u}(\vec{p}') \left\{ g_V \gamma^{\mu} + i \frac{g_T}{2M_N} \sigma^{\mu\nu} q_{\nu} \right\} u(\vec{p}) \varepsilon_{\nu} \vec{\tau} \cdot \vec{\phi}_{\rho}, \\ \mathcal{L}_{\rho NN^*} &= i F_{\rho}(q^2) \bar{u}(\vec{p}') \frac{g_T^*}{M_{N^*} - M_N} \sigma^{\mu\nu} q_{\nu} u(\vec{p}) \varepsilon_{\nu} \vec{\tau} \cdot \vec{\phi}_{\rho},\end{aligned}\quad (8)$$

where $q = p - p'$ denotes the four momentum of the exchanged meson and $\vec{q}_{\alpha N} = (M_N \vec{q} - m_{\alpha} \vec{p}) / (M_N + m_{\alpha})$ the relative meson nucleon three momentum with $\alpha \in \{\pi, \eta\}$. Further, each meson nucleon vertex αNN with $\alpha \in \{\pi, \eta, \rho\}$ contains a form factor of monopole type

$$F_{\alpha}(q^2) = \frac{\Lambda_{\alpha}^2 - m_{\alpha}^2}{\Lambda_{\alpha}^2 - q^2}.\quad (9)$$

The corresponding αNN^* transition vertices with $\alpha \in \{\pi, \eta\}$ are regularized by form factors of the form

$$F_{\alpha}^*(\vec{q}_{\alpha N}^2) = \frac{\Lambda_{\alpha}^{*2}}{\Lambda_{\alpha}^{*2} + \vec{q}_{\alpha N}^2}.\quad (10)$$

For the ρNN^* vertex the same form factor as for ρNN is used. With this meson exchange model the functions M_j appearing in (5) can be written as a sum over the participating mesons

$$M_j = M_j^{(\pi)} + M_j^{(\rho)} + M_j^{(\eta)}.\quad (11)$$

Detailed expressions for $M_j^{(\alpha)}$ $\alpha \in \{\pi, \eta, \rho\}$ are listed in the appendix.

Following the work of [2], the main calculation is based on the assumption that the $NN \rightarrow NN^*$ transition is dominated by ρ exchange. The contribution of π meson exchange to the amplitude is about three times smaller. The η meson with an ηNN coupling $g_{\eta NN}^2/4\pi = 0.4$ from [14] provides only a tiny correction at the level of about 3 %. The ρNN^* coupling constant g_T^* was treated as a free parameter. It was adjusted in such a way that the total cross section in both channels, pp and np , is normalized to the corresponding data with the same normalization factor $C_n < 1$. This factor takes effectively into account the damping of the initial beam via inelastic collisions other than $NN \rightarrow \eta NN$.

The parameters appearing in (8) to (10) are listed in Tables I and II. Those for the αNN couplings, used also in [2] are given in [15], except for $g_{\eta NN}$ which was taken from [14]. The πNN^* and ηNN^* parameters are taken from [16] and [10] as is explained below. With this set of parameters we obtain as normalization factor $C_n = 0.18$, which is appreciably smaller than the value $C_n \approx 0.55$ of [2] and also less than the values 0.23 and 0.2 obtained respectively in [4] and [17]. In view of some obvious limitations adopted here for the production potential, e.g., neglect of direct emission of an η meson by one of the nucleons as well as the contribution of other mesons, we do not put too much significance on this quite small value for the damping factor C_n .

Clearly, the present model is only one of possible ways to parametrize the $NN \rightarrow NN^*$ transition amplitude. As was discussed in [2], the isovector exchange with a dominance of ρ over π exchange is consistent with the observed ratio of about 6.5 of the $np \rightarrow \eta np$ to $pp \rightarrow \eta pp$ cross section [18] as well as with the characteristic $(a - \cos^2 \theta_\eta)$ -dependence of the η angular distribution [19]. For this model the transition with $T = 0$ strongly dominates over $T = 1$ and, among others, results in a large probability of deuteron formation [2] in agreement with experimental results [18]. However, as has been shown in [4] and [5], more sophisticated treatments of the initial state interaction as well as inclusion of genuine two-body meson production mechanisms favour π dominance. Therefore, in order to broaden our theoretical basis, we consider in addition the second type of $NN \rightarrow NN^*$ potential, where the ρ meson is neglected. Another purpose of using such an extreme approximation is to see to which extent the FSI effects depend on the details of the $NN \rightarrow NN^*$ transition. One might anticipate the result that due to the short-range nature of the $NN \rightarrow NN^*$ interaction such a dependence can not be very significant. However, in view of the basic theoretical uncertainties with respect to the production mechanism, this question has to be investigated quantitatively. Indeed, as will be shown below, the sensitivity of FSI effects to the variation of the relative strength of π to ρ exchanges in the production potential, although not very dramatic, results in a variation of FSI effects of about 30 %.

III. RESULTS AND DISCUSSION

Our method of solving the three-body equations is based on separable representations of the driving two-body forces. For the ηN interaction we use the isobar model of [16], where the resonance parametrization of the partial wave amplitudes is fitted to the $\pi N \rightarrow \pi N$, $\pi N \rightarrow \pi \pi N$, and $\pi^- p \rightarrow \eta n$ channels. In particular in the S_{11} channel only the $S_{11}(1535)$ resonance was taken into account. Apart from the original set of S_{11} parameters presented in [16], which gives for the ηN scattering length $a_{\eta N} = (0.25 + i0.16)$ fm, we considered another parametrization listed in Table II, which gives a value twice as large, namely $a_{\eta N} = (0.52 + i0.33)$ fm, and at the same time allows one to describe well the above-listed reactions. More details are given in [20]. These two sets of parameters are used to study the sensitivity of the result to the ηN interaction model.

The NN interaction is included in S , P and D waves in both isospin states, namely 1S_0 , 3P_J ($J = 0, 1, 2$), and 1D_2 waves for $T = 1$ and 3S_1 , 1P_1 , and 3D_J ($J = 1, 2, 3$) for $T = 0$. The corresponding off-shell amplitudes were obtained using the separable representation of the Paris potential from [21]. The remaining higher partial waves of the NN subsystem were taken as plane waves.

The Faddeev equations for the ηNN system were solved only for the states of lowest angular momentum where a relative two-particle S state, either (NN) or (ηN) , is coupled with an S state of the third particle relative to this pair, resulting in the partitions $\eta + (NN)$ or $N + (\eta N)$, respectively. As the explicit calculation shows, in the energy region of current interest, $Q < 60$ MeV, these S waves are almost totally overlapping. The other partial waves were treated perturbatively up to first order in the ηN and NN scattering amplitudes.

The separable representation of the two-body t matrices allows one to reduce the original Faddeev equations to a set of two integral equations in one variable only, presented schematically in Fig. 1. Their structure is identical to the usual Lippmann-Schwinger equation for the two coupled channels $(N + N^*)$ and $(\eta + d)$, where the notation “ d ” is used for the interacting NN subsystem. The reaction amplitude M is then expressed in terms of the auxiliary quasi-two-body amplitudes X_d and X_{N^*} as is presented in the same figure. With respect to the application of three-body scattering theory to reactions with three free particles in the final state we refer to [22]. Some technical points concerning the ηNN problem are described in [7].

We begin the discussion of our results with the total cross section shown in Figs. 2 and 3 for $pp \rightarrow \eta pp$ and

$np \rightarrow \eta np$, respectively. As already noted, the three-body result is normalized to the data at one point, namely at $Q = 36$ MeV to $\sigma = 5.6 \mu\text{b}$ using PROMISE-WASA data [23] for pp and to $\sigma = 35 \mu\text{b}$ with CELSIUS data [18] for np . Of course, the ratio between the different curves is fixed by the model. Therefore, apart from the fact that the same normalization factor is used for both reactions, the only nontrivial result in Figs. 2 and 3 is the energy dependence of the cross sections. For obvious reasons, detailed experimental data are available for the $pp \rightarrow \eta pp$ reaction only, which, however, is much more difficult for a theoretical study of the near threshold region because of the Coulomb interaction between the protons. In the present work we have not included the Coulomb force, which fact, of course, hampers to some extent a quantitative comparison with the data. Nevertheless, the results shown in Figs. 2 and 3 allows us to draw the following conclusions:

The three-body model reproduces quite well the energy dependence of the experimental cross section in the pp channel. The deviation very close to threshold must primarily be ascribed to the neglect of Coulomb repulsion. As for the np channel, the agreement with the data of [18] appears to be less satisfactory. The theory exhibits a more flat form of the cross section. Clearly, for a meaningful conclusion about the quality of the present model a greater amount of data is needed, especially in the vicinity of the threshold.

The first-order calculation, where the FSI is reduced to only ηN and NN rescatterings, does not reproduce the form of the $pp \rightarrow \eta pp$ cross section as predicted by the three-body treatment and also observed in the experiment. As was noted in the introduction, it is expected that the leading terms associated with ηN and NN rescatterings do not constitute a reliable approximation of the whole multiple scattering series, due to the slow convergence of this series in the vicinity of the virtual ηNN pole. The strong difference between the first order and the exact three-body calculation even at $Q = 60$ MeV demonstrates the crucial importance of higher order terms. We consider this result as a direct evidence for the fact that a three-body approach is definitely needed for a correct treatment of the ηNN interaction. Thus, the first-order approximation, although seemingly reasonable in view of the weak ηN interaction as compared to the NN one, is in general not relevant.

The question of a correct treatment of FSI in η production is closely related to the relative fraction of S waves in the final state. As was mentioned above, in accordance with the short range hypothesis for the η production mechanism, the S waves in the ηNN system are expected to provide the major part of the cross section in the threshold region, thus making the FSI effect to be of particular importance in this reaction. In this context it is instructive to compare the relative contribution of the S waves to the total cross sections of $\gamma d \rightarrow \eta np$ and $pp \rightarrow \eta pp$. The results of the IA for both processes are presented in Fig. 4, where the 1S_0 s contribution [24] is shown separately. Because of the relatively long range nature of the mechanism for η photoproduction on the deuteron, the contribution of higher partial waves in the final state increases rapidly and already at the energy $Q = 60$ MeV the S wave provides only a 10 % fraction of the total cross section. In contrast to this, the 1S_0 s configuration strongly dominates the reaction $pp \rightarrow \eta pp$ in the whole energy region, so that even at $Q = 60$ MeV it produces about 77 % of the cross section. In conclusion, the role of the final state interaction depends not only on the phase space available for the final particles (which is the same for both reactions) but much more crucially on the range of the primary $NN \rightarrow NN^*$ transition interaction.

On the right panel of Fig. 2 the dependence of the results on the model ingredients is exhibited. Firstly, we would like to note a visible sensitivity of the cross section to the choice of which meson exchange governs the production potential. Namely, π dominance tends to make the form of the total cross section more convex as compared to the full curve where ρ exchange prevails, whereas the IA gives in both cases practically indistinguishable results except for the normalization factor C_n . Using a weaker ηN interaction from [16], we obtain, as expected, a weaker influence of FSI as is shown by the dash-dotted line in the right panel of Fig. 2.

In Fig. 5 we compare our calculation for the pp invariant mass distribution with the COSY-11 [9] and TOF [13] data. At the excess energy $Q = 15.5$ MeV the three-body result was normalized to the experimental integrated cross section $\sigma = 3.24 \mu\text{b}$ of [9]. The distribution at $Q = 41$ MeV is given in arbitrary units and the theoretical full curve was normalized to the area enclosed by the data points. For a lower excess energy $Q = 15.5$ MeV one finds a reasonable agreement of the three-body calculation with the data, although one notes a systematic slight underestimation of the experimental cross section in the region above $M_{pp}^2 = 3.54 (\text{GeV})^2$. At least some part of the deviation stems again from an overestimation of the pp interaction effect at the lower end of the spectrum due to the neglect of the Coulomb force. In view of the overall normalization, inclusion of the Coulomb repulsion would reduce the 1S_0 peak near $M_{pp} = 2M_N$, and would enhance the other part of the distribution.

However, at the higher excess energy $Q = 41$ MeV the shape of the theoretical distribution is in strong disagreement with the data. In particular, the broad maximum around $M_{pp}^2 = 3.62 \text{ GeV}^2$ is not explained. Of course, in order to reach at a definite conclusion, the Coulomb interaction must be included in addition, but it is very unlikely that this would have such a strong effect as to explain the shape. Moreover, our results are at variance with those of [12] where an appreciable contribution of higher angular momentum states in the pp subsystem is predicted, whereas our calculation does not indicate a sizeable influence from P and D partial NN waves. The corresponding contributions can be estimated by comparison of the full and the dash-dotted curves in Fig. 5. In the latter calculation only the lowest 1S_0 s configuration in the ηNN final state was included.

On the other hand, it is worth to underline the importance of the NN tensor force, which increases quite appreciably the transition to the 3S_1 state from an intermediate 3D_1 after η production. The relevance of this intermediate 3D_1 state is related to the strong momentum transfer accompanying η production and emphasizing the high momentum components of the NN wave function. One of the consequences of this fact is that the enhancement by the NN interaction for the $T = 0$ transition is even slightly stronger than that for $T = 1$. This result is at variance with [2], where a ratio of the enhancement factors of $T = 1$ to $T = 0$ of 1.85 at relative NN momenta $p_r > 0.5 \text{ fm}^{-1}$ was found. According to our results in Fig. 6, this ratio is reduced from 1.35 to only 0.98 at $p_r = 0.5 \text{ fm}^{-1}$ if the transition $^3D_1 \rightarrow ^3S_1$ is included.

In Fig. 7 the calculated distribution with respect to the η kinetic energy T_η in $pp \rightarrow \eta pp$ is plotted together with the CELSIUS data [19]. One readily notes quite a good agreement except for a very small region close to the maximal kinetic energy. We do not consider this discrepancy as a serious defect because, as was noted in [19], some fraction of the events must have been lost. Furthermore, we would like to point out that the data of the pp mass distribution at $Q = 41 \text{ MeV}$ in the right panel of Fig. 5 appears to be in conflict with the data at $Q = 37 \text{ MeV}$ in the right panel of Fig. 7. The latter increases monotonically with meson energy except very close to the maximal kinetic energy T_η , whereas the TOF results for $d\sigma/dM_{pp}^2$ in Fig. 5 exhibit a pronounced broad maximum at intermediate pp masses. In view of the simple relation

$$\frac{d\sigma}{dT_\eta} = -2W \frac{d\sigma}{dM_{pp}^2}, \quad (12)$$

one would expect on the other hand a similar behaviour for both distributions, because the small difference in the energies can hardly result in a very different form of the spectrum. Thus new experimental data for the T_η and/or M_{pp}^2 distributions in the region $Q = 37 - 41 \text{ MeV}$ are needed in order to resolve this discrepancy.

Finally, we present in Fig. 8 the angular distribution of an emitted proton for two excess energies. The dominance of ρ exchange in the production mechanism leads to a pronounced isotropy of the cross sections. This becomes apparent by comparison with the angular distributions using a pure π exchange. They exhibit a much stronger angular dependence with a more pronounced peaking at forward and backward directions, which is consistent with a more peripheral character of the π exchange mechanism. In general, the proton angular distribution with a weak $\cos^2 \theta_p$ dependence is consistent with the almost isotropic form of the experimental results of [13], although the observed magnitude at $Q = 41 \text{ MeV}$ is overestimated by about 20 %. Furthermore, one should keep in mind the pronounced disagreement between theory and the TOF data for the M_{pp}^2 spectrum at the same energy (see Fig. 5). With respect to the η angular distribution, we did not analyze it here in view of its obvious sensitivity to higher ηN resonances, predominantly $D_{13}(1520)$, which were omitted in the present calculation.

IV. CONCLUSIONS

In the present paper we have investigated η production in NN collisions in the near threshold region. The main attention was focussed on the understanding of the role of FSI, which is expected to strongly influence the reaction dynamics near threshold. We believe that in conjunction with previous work [1, 2, 3, 4, 5] the present study was necessary in order to establish a unified picture of this reaction. In particular, it can be quite useful for the planning and analysis of future experiments. From our results we draw the following conclusions:

- (i) The three-body treatment of the ηNN interaction provides a satisfactory, quantitative explanation of the energy dependence of the total cross section for $pp \rightarrow \eta pp$. However, the dependence of the results on the details of the $NN \rightarrow NN^*$ transition introduces some uncertainty. In particular, assuming a pion exchange dominance in the production potential leads to stronger energy dependence of the cross section and requires, therefore, a weaker ηN interaction in order to bring the theory into agreement with the data.
- (ii) There is a discrepancy between our results and the data of [13] for the M_{pp}^2 distribution at a c.m. excess energy $Q = 41 \text{ MeV}$. Namely, the broad peak of the data is not described by the theory. Comparing to other theoretical work, we do not reproduce the result of [12], where this broad structure is explained by the contribution of higher partial waves in the NN subsystem. On the contrary, according to our findings the contribution of P and D waves in the final pp subsystem plays a minor role only, at least in the region up to $Q = 60 \text{ MeV}$ considered in the present work.
- (iii) Even close to threshold, where the final NN system is predominantly in an S wave state, the tensor NN force in the $T = 0$ channel must be taken into account. As we have shown, the intermediate transition to a 3D_1 configuration with subsequent rescattering into the 3S_1 state enhances sizeably the NN interaction effect in the triplet state.

Before concluding, we would like to note that the sensitivity of the FSI effect to the $NN \rightarrow NN^*$ transition mentioned in (i) indicates that in principle the short range part of the final state wave function must be calculated more thoroughly than is done here. Obviously, the most straightforward way would be a three-body treatment of

the whole $NN \rightarrow \eta NN$ process without restriction to the final state. However it seems to be very difficult in view of the great amount of channels which have to be included in such an approach, not to mention the pure theoretical ambiguity in treating the NN system within the three-body formalism. On the other hand, one can expect that short range mechanisms may be included perturbatively. For example, the πNN configurations could be considered in first order only (apart from the driving meson exchange potential) by including the additional mechanism where a pion, created in an NN collision, produces in turn an η via rescattering on one of the nucleons. Clearly, such an approach, which would allow us to adopt the same FSI concept, is practically much easier to manage than a rigorous solution of the three-body coupled channel model.

Acknowledgments

This work was supported by the Deutsche Forschungsgemeinschaft (SFB 443).

Appendix A

In this appendix we give the explicit expressions for the amplitudes $M_j^{(\alpha)}$, $\alpha \in \{\pi, \eta, \rho\}$ for the transition $NN \rightarrow NN^*$ determining the transition matrix element $T_{NN^*}(\vec{p}, \vec{p}')$. The latter was defined in the c.m. system with \vec{p} and \vec{p}' denoting the momenta of the initial and final states, respectively. In the following expressions we have introduced the notations:

$$\begin{aligned} E &= \sqrt{p^2 + M_N^2} = \frac{W}{2}, & E' &= \sqrt{p'^2 + M_N^2}, & E^* &= \sqrt{p'^2 + M_{N^*}^2}, \\ \epsilon &= E + M_N, & \epsilon' &= E' + M_N, & \epsilon^* &= E^* + M_{N^*}, \\ P_\mu &= (E + E', \vec{p} + \vec{p}'), & P_\mu^* &= (E + E^*, -\vec{p} - \vec{p}'), & \Delta M^* &= M_{N^*} - M_N, \\ \vec{q}'^{(*)} &= \frac{\vec{p}}{\epsilon} - \frac{\vec{p}'}{\epsilon'^{(*)}}, & \vec{r}'^{(*)} &= \frac{\vec{p}}{\epsilon} + \frac{\vec{p}'}{\epsilon'^{(*)}}. \end{aligned} \quad (\text{A1})$$

The expressions for ρ exchange are obtained by using the on-shell Gordon decomposition of the nucleon current

$$\bar{u}(\vec{p}') \gamma_\mu u(\vec{p}) = \frac{1}{2M_N} \bar{u}(\vec{p}') [(p_\mu + p'_\mu) - i\sigma_{\mu\nu}(p_\nu - p'_\nu)] u(\vec{p}) \quad (\text{A2})$$

and the analogous relation for the ρNN^* coupling. In the present paper the invariant energy ω_{N^*} of the N^* or ηN subsystem was determined according to the spectator on-shell scheme

$$\omega_{N^*} = W - M_N - \frac{p^2}{2} \left(\frac{1}{M_N} + \frac{1}{M_N + m_\eta} \right), \quad (\text{A3})$$

which is consistent with the nonrelativistic three-body treatment of the ηNN system. Furthermore, this choice of ω_{N^*} justifies the use of the Gordon decomposition for the tensor part in the ρNN coupling since in this case the nucleon remains on-shell after emission of a ρ meson. The only approximation, whose validity is not justified is the Gordon relation for the ρNN^* coupling. We believe, however, that, since the coupling constant g_T^* is treated here as a free parameter, it is a reasonable approximation.

Using the vertices (8) one finds the following contributions from π , η , and ρ meson exchange:

(i) π meson exchange:

$$M_j^{(\pi)} = \frac{\epsilon}{2M_N} \sqrt{\frac{\epsilon' \epsilon^*}{4M_N M_{N^*}}} g_{\pi NN} g_{\pi NN^*} \frac{F_\pi(q^2) F_\pi^*(\vec{q}_{\pi N}^2)}{q^2 - m_\pi^2} F_j, \quad (\text{A4})$$

where

$$F_{1(2)} = \pm \frac{1}{\epsilon^{(\prime)}} \left(1 - \frac{\vec{p} \cdot \vec{p}'}{\epsilon \epsilon^*} \right), \quad (\text{A5})$$

$$F_{3(4)} = 0, \quad (\text{A6})$$

$$F_{6(5)} = \mp \frac{\vec{q} \cdot \vec{p}^{(\prime)}}{\epsilon \epsilon^*}, \quad (\text{A7})$$

$$F_{7(8)} = \pm \frac{1}{\epsilon \epsilon^* \epsilon^{(\prime)}}. \quad (\text{A8})$$

(ii) η meson exchange: Since the formal expressions are the same as for π exchange except for a replacement of coupling constants and meson mass, we do not need to repeat them here:

$$M_j^{(\eta)} = M_j^{(\pi)} \Big|_{\pi \rightarrow \eta} . \quad (\text{A9})$$

(iii) ρ meson exchange:

$$M_j^{(\rho)} = -\frac{\epsilon}{2M_N} \sqrt{\frac{\epsilon' \epsilon^*}{4M_N M_{N^*}}} \frac{g_T^* F_\rho^2(q^2)}{q^2 - m_\rho^2} F_j , \quad (\text{A10})$$

where

$$F_{2(1)} = \mp(g_V + g_T) \frac{\vec{q}' \cdot \vec{p}^{(\prime)}}{\epsilon \epsilon^*} \quad (\text{A11})$$

$$F_3 = \frac{g_V + g_T}{\epsilon} \left[-2 - \frac{\vec{p}' \cdot \vec{r}^*}{\epsilon'} + \left(1 + \frac{\vec{p} \cdot \vec{p}'}{\epsilon \epsilon'} \right) \frac{P_0^*}{\Delta M^*} + \frac{\vec{r}' \cdot \vec{P}}{\Delta M^*} \right] + \frac{g_T}{2M_N \epsilon} \left(1 - \frac{\vec{p} \cdot \vec{p}'}{\epsilon \epsilon'} \right) \left[W + \epsilon' + \frac{p'^2}{\epsilon^*} - \frac{P^\mu P_\mu^*}{\Delta M^*} \right] , \quad (\text{A12})$$

$$F_4 = \frac{g_V + g_T}{\epsilon^*} \left[-1 - \frac{\epsilon^*}{\epsilon'} - \frac{\vec{p} \cdot \vec{r}'}{\epsilon} - \left(1 + \frac{\vec{p} \cdot \vec{p}'}{\epsilon \epsilon'} \right) \frac{P_0^*}{\Delta M^*} - \frac{\vec{r}' \cdot \vec{P}}{\Delta M^*} \right] + \frac{g_T}{2M_N \epsilon^*} \left(1 - \frac{\vec{p} \cdot \vec{p}'}{\epsilon \epsilon'} \right) \left[W + \epsilon + \Delta M^* + \frac{p^2}{\epsilon} + \frac{P^\mu P_\mu^*}{\Delta M^*} \right] \quad (\text{A13})$$

$$F_5 = -\frac{g_V + g_T}{\epsilon \epsilon'} \left[2\epsilon' + \frac{\vec{p} \cdot \vec{p}'}{\epsilon} \left(1 - \frac{\epsilon'}{\epsilon^*} \right) + \frac{2p'^2}{\epsilon^*} - \frac{2(W + M_N)}{(\Delta M^*)} \vec{p}' \cdot \vec{q}^* \right] - \frac{g_T}{2M_N \epsilon \epsilon'} \left[\frac{\vec{p} \cdot \vec{p}'}{\epsilon} \left(W + \epsilon' + \frac{p'^2}{\epsilon^*} \right) + \frac{p'^2}{\epsilon^*} \left(W + \epsilon' + \Delta M^* + \frac{p^2}{\epsilon} \right) - \vec{p}' \cdot \vec{q}^* \frac{P^\mu P_\mu^*}{\Delta M^*} \right] \quad (\text{A14})$$

$$F_6 = \frac{g_V + g_T}{\epsilon \epsilon'} \left[2\epsilon + \frac{p^2}{\epsilon} \left(1 + \frac{\epsilon'}{\epsilon^*} \right) - \frac{2(W + M_N)}{\Delta M^*} \vec{p} \cdot \vec{q}^* \right] + \frac{g_T}{2M_N \epsilon \epsilon'} \left[\frac{\vec{p} \cdot \vec{p}'}{\epsilon^*} \left(W + \epsilon + \Delta M^* + \frac{p^2}{\epsilon} \right) + \frac{p^2}{\epsilon} \left(W + \epsilon' + \frac{p'^2}{\epsilon^*} \right) - \vec{p}' \cdot \vec{q}^* \frac{P^\mu P_\mu^*}{\Delta M^*} \right] \quad (\text{A15})$$

$$F_7 = \frac{g_V + g_T}{\epsilon^2 \epsilon'} \left[1 + \frac{\epsilon'}{\epsilon^*} - \frac{2(W + M_N)}{\Delta M^*} \right] + \frac{g_T}{2M_N \epsilon^2 \epsilon'} \left[W + \epsilon' + \frac{p'^2}{\epsilon^*} - \frac{P^\mu P_\mu^*}{\Delta M^*} \right] \quad (\text{A16})$$

$$F_8 = \frac{g_V + g_T}{\epsilon \epsilon' \epsilon^*} \left[2 + \frac{2(W + M_N)}{\Delta M^*} \right] + \frac{g_T}{2M_N \epsilon \epsilon' \epsilon^*} \left[W + \epsilon + \Delta M^* + \frac{p^2}{\epsilon} + \frac{P^\mu P_\mu^*}{\Delta M^*} \right] \quad (\text{A17})$$

-
- [1] E. Gedalin, A. Moalem, and L. Razdolskaja, Nucl. Phys. A **634**, 368 (1998).
 - [2] G. Fäldt and C. Wilkin, Phys. Scripta **64**, 427 (2001).
 - [3] M.T. Peña, H. Garcilazo, and D.O. Riska, Nucl. Phys. A **683**, 322 (2001).
 - [4] K. Nakayama, J. Speth, and T.S.H. Lee, Phys. Rev. C **65**, 045210 (2002).
 - [5] V. Baru *et al.*, Phys. Rev. C **67**, 024002 (2003).
 - [6] A. Deloff, nucl-th/0309059.
 - [7] A. Fix and H. Arenhövel, Nucl. Phys. A **697**, 277 (2002); Phys. Lett. B **492**, 32 (2000).
 - [8] A. Fix and H. Arenhövel, Z. Phys. A **359**, 427 (1997).
 - [9] P. Moskal *et al.*, nucl-ex/0307005.
 - [10] A. Fix and H. Arenhövel, nucl-th/0305098.
 - [11] A. Fix and H. Arenhövel, Eur. Phys. J. A **9**, 119 (2000).
 - [12] K. Nakayama *et al.*, nucl-th/0302061.
 - [13] M. Abdel-Bary *et al.*, Eur. Phys. J. A **16**, 127 (2003).
 - [14] L. Tiator, C. Bennhold, and S.S. Kamalov, Nucl. Phys. A **580**, 455 (1994).
 - [15] R. Machleidt, Phys. Rev. C **63**, 024001 (2001).
 - [16] C. Bennhold and H. Tanabe, Nucl. Phys. A **530**, 625 (1991).
 - [17] H. Garcilazo and M.T. Peña, Phys. Rev. C **66**, 034606 (2002).
 - [18] H. Calén *et al.*, Phys. Rev. C **58**, 2667 (1998).

- [19] H. Calén *et al.*, Phys. Lett. B **458**, 190 (1999).
- [20] A. Fix and H. Arenhövel, nucl-th/0302050.
- [21] J. Haidenbauer and W. Plessas, Phys. Rev. C **30**, 1822 (1984).
- [22] E. W. Schmid and H. Ziegelmann, *The Quantum Mechanical Three-Body Problem* (Friedrich Vieweg & Sohn, Braunschweig, 1974)
- [23] H. Calén *et al.*, Phys. Lett. B **366**, 39 (1996).
- [24] We use the notation $^{2s+1}L_j l$ for states of the $(\eta + NN)$ partition.

TABLE I: Coupling constants and form factor parameters of the αNN vertices of (8).

$\frac{g_{\pi NN}^2}{4\pi}$	Λ_π [GeV]	$\frac{g_{\eta NN}^2}{4\pi}$	Λ_η [GeV]	$\frac{g_V^2}{4\pi}$	$\frac{g_T^2}{4\pi}$	Λ_ρ [GeV]
14.4	1.7	0.4	1.5	0.84	31.25	1.4

TABLE II: The same as in Table I for the αNN^* vertices.

$\frac{g_{\pi NN^*}}{\sqrt{3}}$	Λ_π^* [GeV]	$g_{\eta NN^*}$	Λ_η^* [GeV]	g_T^*
1.45	0.404	2.00	0.695	1.7

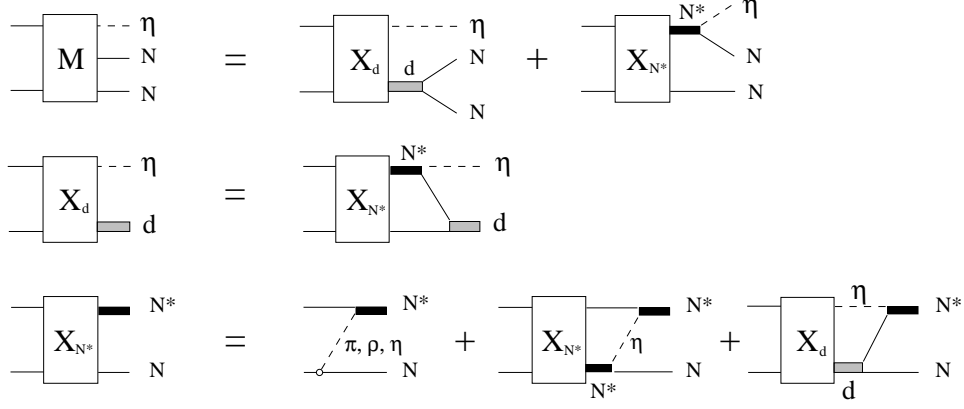


FIG. 1: Diagrammatic representation of the three-body integral equations for the reaction $NN \rightarrow \eta NN$.

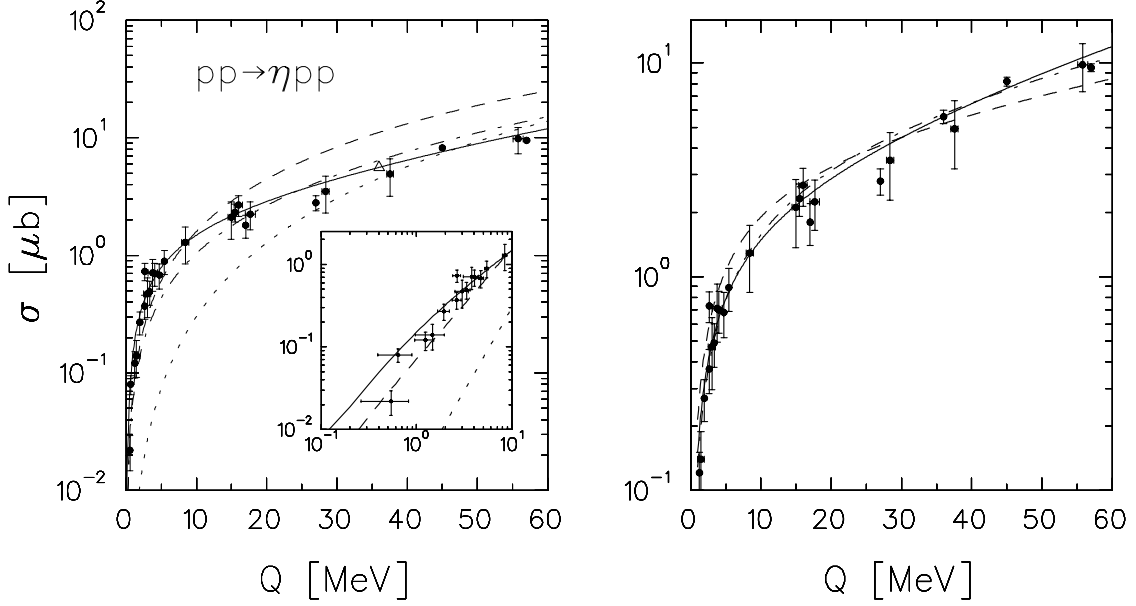


FIG. 2: Left panel: Total cross section for $pp \rightarrow \eta pp$. Notation of curves: dotted: impulse approximation; dashed: rescattering in two-body subsystems only; dash-dotted: rescattering in NN subsystem only; full: three-body calculation. Data from compilation [9]. Open triangle: normalization point $(Q, \sigma) = (36, 5.6)$ from [23]. Inset shows near-threshold region. Right panel: Dependence of three-body result on model ingredients. Notation of curves: solid identical to the one in the left panel; dashed: without ρ exchange in production potential; dash-dotted: calculation with $S_{11}(1535)$ parametrization from [16] with weaker ηN interaction, $a_{\eta N} = (0.25 + i0.16)$ fm, and π dominated $NN \rightarrow NN^*$ potential.

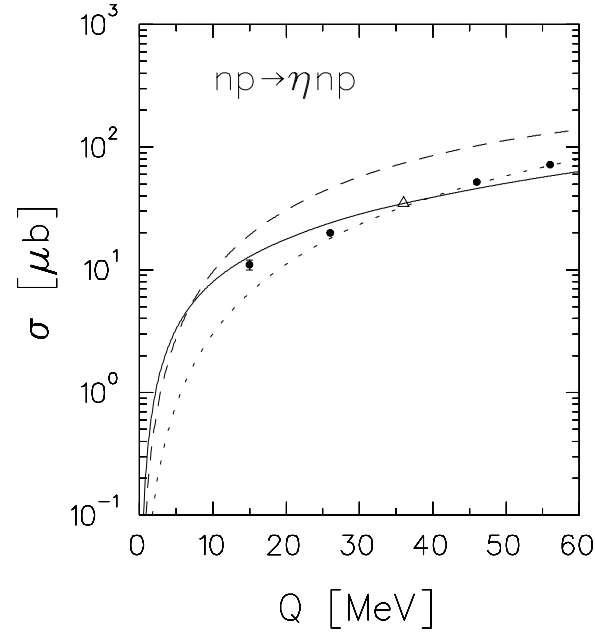


FIG. 3: Same as the left panel of Fig. 2 but for $np \rightarrow \eta np$. Data from [18].

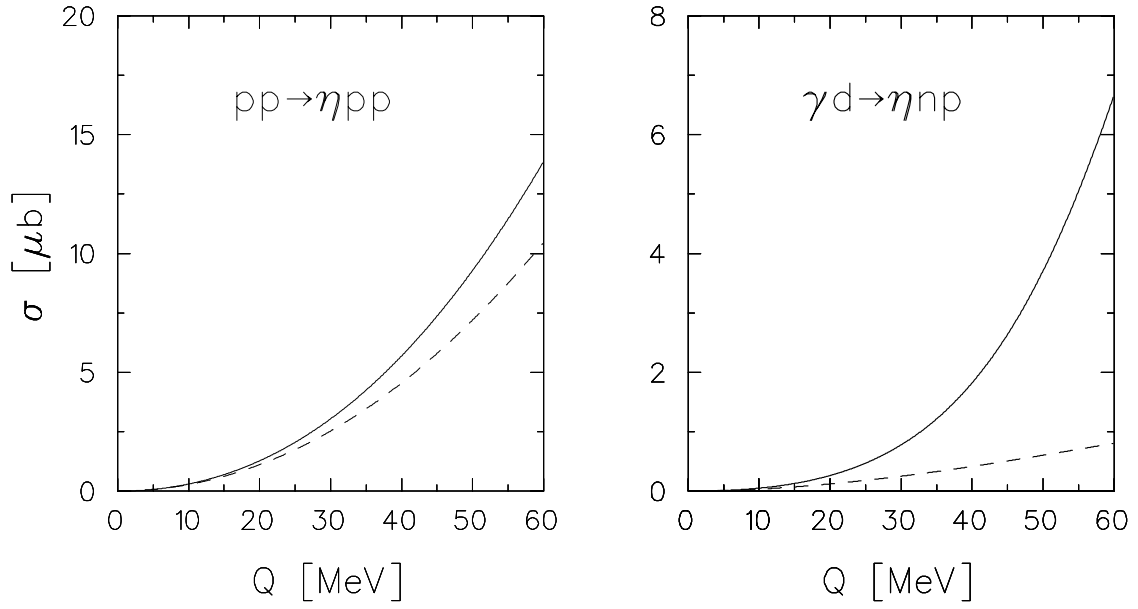


FIG. 4: Total cross sections for $pp \rightarrow \eta pp$ (left panel) and $\gamma d \rightarrow \eta np$ (right panel) calculated in the impulse approximation. Dashed lines include only 1S_0 wave in the final state.

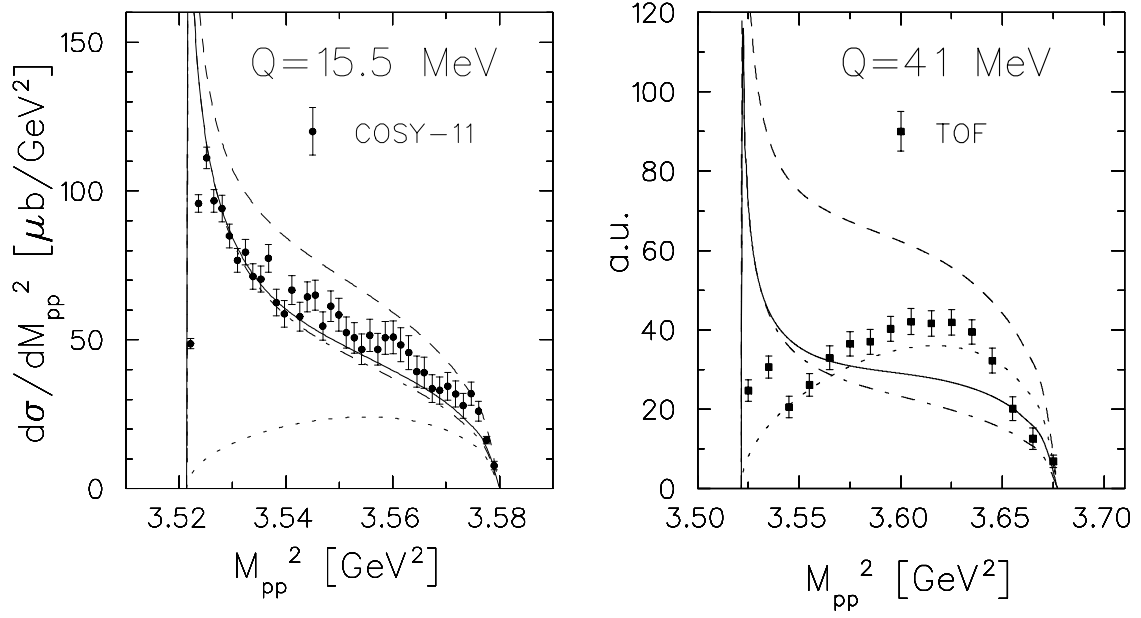


FIG. 5: Distribution of squared pp invariant mass in $pp \rightarrow \eta pp$. Notation of curves as in the left panel of Fig. 2. The dash-dotted curve is obtained with a pure 1S_0s final state. Data at $Q = 15.5$ MeV are from [9] and at $Q = 41$ MeV from [13].

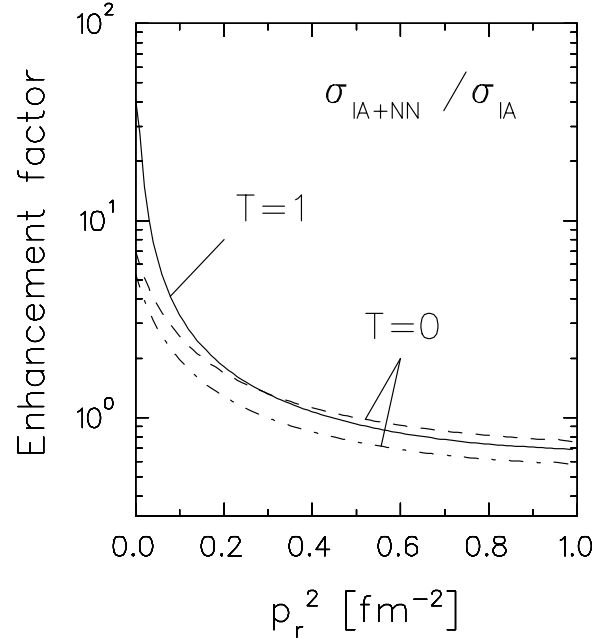


FIG. 6: Enhancement factors associated with the NN interaction in $T = 0$ and $T = 1$ channels as function of the squared relative NN momentum. The dashed and dash-dotted curves are obtained with and without inclusion of the $^3D_1 \rightarrow ^3S_1$ transition, respectively.

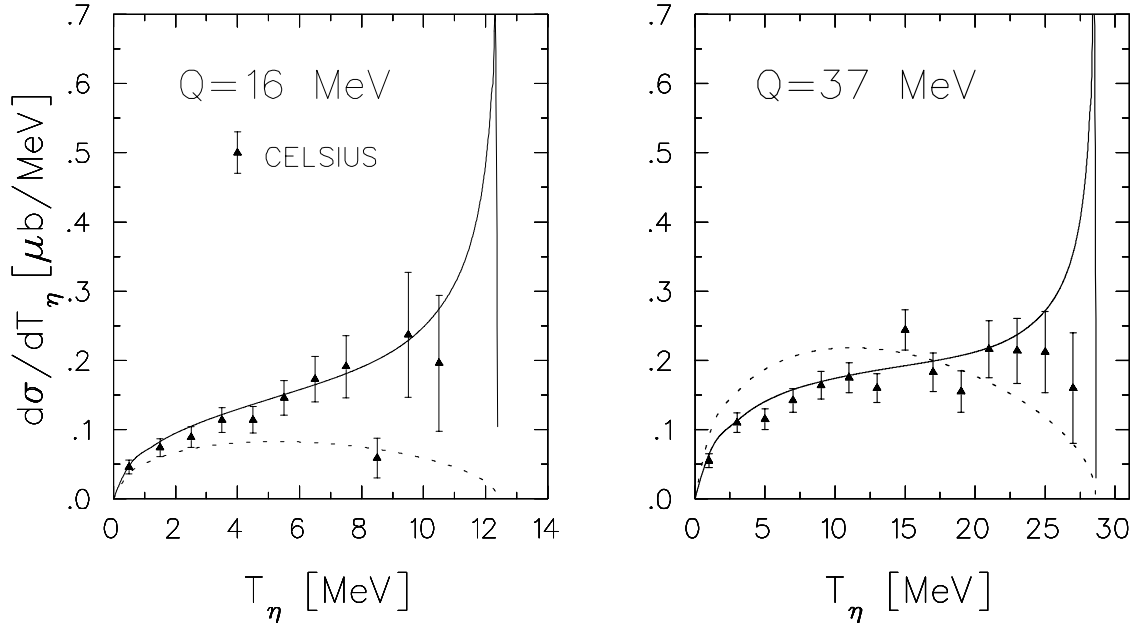


FIG. 7: η meson spectrum for $pp \rightarrow \eta pp$ as a function of η kinetic energy T_η . Solid and dotted curves show respectively the three-body model and IA predictions. Data from [19].

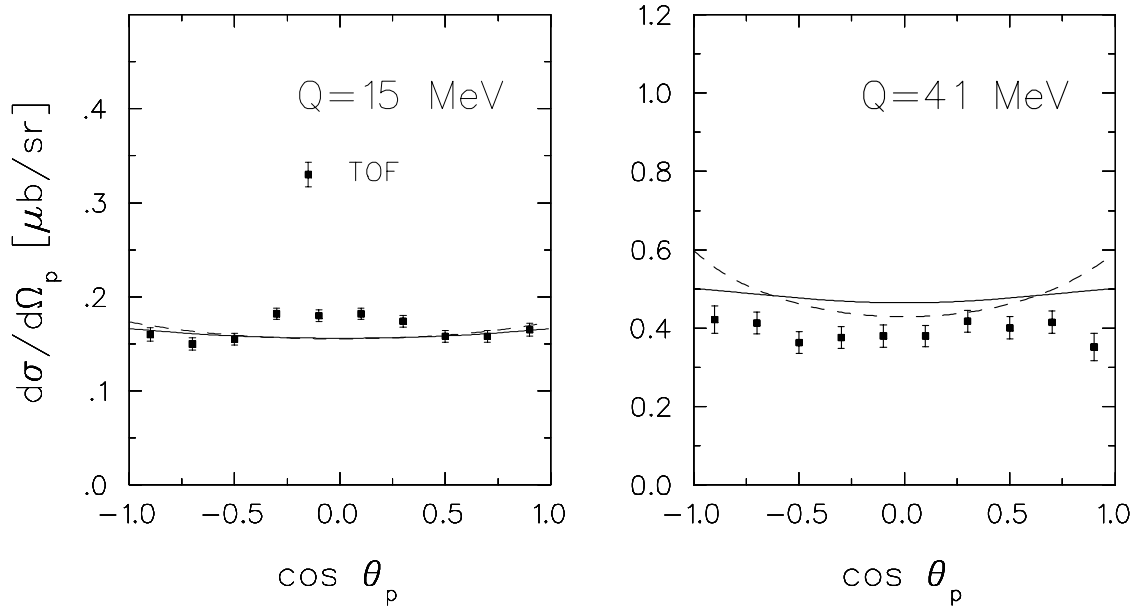


FIG. 8: Angular distribution of protons in $pp \rightarrow \eta pp$. In the dashed curves only π and η meson exchange is included in the production potential. Data from [13].